CHEMPHYSCHEM

DOI: 10.1002/cphc.201100327

Quantitative Study of Non-Covalent Interactions at the Electrode–Electrolyte Interface Using Cyanide-Modified Pt(111) Electrodes

María Escudero-Escribano,[a] Martín E. Zoloff Michoff,[b] Ezequiel P. M. Leiva,[b] Nenad M. Marković,[c] Claudio Gutiérrez,[a] and Ángel Cuesta*[a]

Due to their generally very weak interaction with metal surfaces, the influence of cations on the properties of the electrochemical double layer and on the processes occurring at the electrode–electrolyte interface has traditionally received little attention. However, cations can become attached to the electrode surface through non-covalent interactions (such as hydrogen bonds, ionic bonds, van der Waals forces and hydrophobic interactions, which do not involve the sharing of pairs of electrons[1,2]) with chemisorbed species, affecting the structure and the properties of the interface and, hence, influencing the processes occurring at the electrochemical double layer, as has been shown for some important electrocatalytic processes, such as the methanol oxidation reaction (MOR)[3] and the oxygen reduction reaction (ORR).[3,4] The effect of alkaline metal cations (M^+) on some electrocatalytic reactions in alkaline solution has been recently studied by Strmcnik et al.,[3] who demonstrated that non-covalent interactions between $M^+(H_2O)_x$ and OH_{ad} may affect the surface reactivity, due to the formation of OH_{ad}–$M^+(H_2O)_x$ clusters which effectively block oxygen adsorption. The effect of alkaline metal cations on the cyclic voltammogram (CV) of Pt(111) electrodes in sulfuric acid solutions has also been studied by the Alicante group.[5,6]

Cyanide adsorbs spontaneously and irreversibly on Pt(111) through its carbon atom, with the nitrogen atom facing the solution,[7–9] forming an ordered $(2\sqrt{3}\times2\sqrt{3})R30^\circ$ structure[9–11] (see the Supporting Information, Figure S1). As a consequence, trigonal adsorption and reaction sites are lacking on cyanide-modified Pt(111) electrodes while, at the same time, the uncovered Pt atoms in the troughs separating the hexagonal CN rings remain unaffected.[12–14] Thanks to this peculiar property, we have successfully used cyanide-modified Pt(111) electrodes as model surfaces to investigate the role of atomic ensembles in electrocatalysis[14–16] and to develop new concepts for the rational design of cathode catalysts for the ORR in phosphoric acid fuel cells (or in any environments containing strongly adsorbing tetrahedral anions, like the proton exchange membrane fuel cells, PEMFCs).[4] Herein we present a combined theoretical and experimental study of non-covalent interactions between alkaline metal cations and cyanide-modified Pt(111) electrodes, aimed at deepening our understanding of the factors governing non-covalent interactions in surface electrochemistry and at highlighting their often neglected importance.

The CV of cyanide-modified Pt(111) electrodes in acidic solutions ($HClO_4$, H_2SO_4 and H_3PO_4) has been studied previously.[4,12,13] It has been shown that the cyanide adlayer on Pt(111) is remarkably stable, no change being observed in the CVs of the cyanide-covered electrode upon repetitive cycling between 0.05 and 1.10 V versus the reversible hydrogen electrode (RHE). A very interesting aspect is the 0.20 V positive shift of the onset of hydrogen adsorption [corresponding to a ca. 19 kJ mol^{-1} more negative $\Delta G_0(H_{upd}, \theta=0)$], as compared with unmodified Pt(111) electrodes,[4,14] this probably being the only example of a positive shift of the onset potential for H_{upd} formation. This behavior has been attributed to the formation of $(CN_{ad})_x$-H clusters due to non-covalent (electrostatic) interactions between the negative end of the CN_{ad} dipole and the oppositely charged H^+.[4] CN_{ad} acts as an inert site blocker (third body effect)[4,12–16] and, hence, will not affect the energetics of the Pt–H_{upd} bond. The analysis of the density of states (DOS) for the topmost Pt atoms (Figure 1), shows that the DOS of the Pt atoms directly bonded to the CN_{ad} is shifted to lower energies, this being consistent with a strong bonding (the binding energy was calculated to be −3.19 eV per CN). On the other

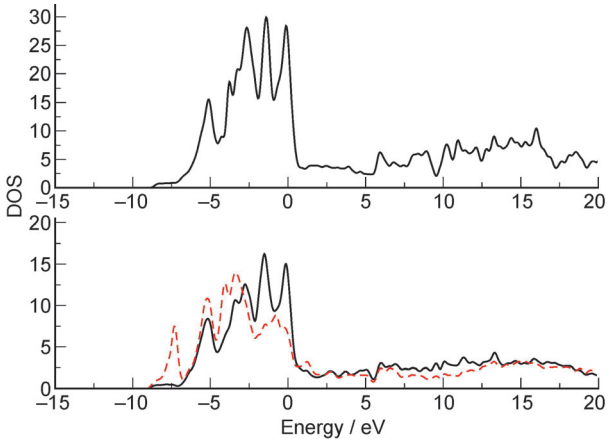

Figure 1. a) DOS for the Pt atoms of a clean (111) surface. b) DOS for the topmost Pt atoms of the cyanide-modified (111) surface, (——) Pt atoms not bonded to a CN, and (-----) Pt atoms bonded to a CN molecule. Energies are referred to the corresponding Fermi level energy.

[a] M. Escudero-Escribano, Prof. C. Gutiérrez, Dr. Á. Cuesta
Instituto de Química Física "Rocasolano"
CSIC, C. Serrano, 119, 28006 Madrid (Spain)
Fax: (+34) 915642431
E-mail: a.cuesta@iqfr.csic.es

[b] M. E. Zoloff Michoff, Prof. E. P. M. Leiva
Facultad de Ciencias Químicas
Universidad Nacional de Córdoba, Córdoba (Argentina)

[c] Prof. N. M. Marković
Materials Science Division, Argonne National Laboratory
Argonne, Illinois 60439 (USA)

Supporting information for this article is available on the WWW under http://dx.doi.org/10.1002/cphc.201100327.

hand, the DOS of the atoms which are not bonded to the adsorbed CN molecules remains nearly identical to the DOS of the Pt atoms of the clean (111) surface, supporting the notion that CN_{ad} acts as an inert site blocker. Accordingly, the positive shift in the onset potential for hydrogen adsorption on Pt indicates that forming $(CN_{ad})_x$-H clusters is more favoured than forming a Pt-H_{upd} bond.

The electronic density and the electrostatic potential for a negatively charged particle averaged in the plane parallel to the surface were also calculated (see the Supporting Information, Figure S2). The difference in electrostatic potential between the CN-covered surface and the clean Pt(111) surface is 2.86 V, with the former being *more negative* than the latter. This implies that the work function of the modified surface is 8.77 eV [i.e. 2.86 eV higher than that of Pt(111), 5.93 eV[17]], and explains the avidity of the modified surface for positively charged particles, such as the cations present in solution (see below).

Any cation in solution can be expected to interact with the negative end of the CN_{ad} dipole on the surface of a cyanide-modified Pt(111) electrode, binding some of the CN_{ads} groups, that will not be available for the formation of $(CN_{ad})_x$-H clusters, and provoking a change in the shape and/or position of the hydrogen-adsorption region in the CV of cyanide-modified Pt(111) electrodes. Such an effect is illustrated in Figures S3–S6 of the Supporting Information, which show the variations observed in the cyclic voltammogram of a cyanide-modified Pt(111) electrode as the concentration of Li^+, Na^+, K^+ or Cs^+ increases.

In Figure 2 we have plotted the potential at which a given coverage by $(CN_{ad})_x$-H clusters has been achieved (i.e., at which a given adsorption charge has crossed the interface) as a function of the logarithm of the cation concentration for Li^+, Na^+, K^+, and Cs^+. Please note that while for the cases of Li^+, Na^+ and K^+ we have plotted the variation of the potential of the peak occurring at 0.48 V in the absence of cations (corresponding to a charge of ca. 20 $\mu C\,cm^{-2}$), in the case of Cs^+ this peak is not clearly defined (see Supporting Information, Figure S6), and the peak at 0.32 V (corresponding to a charge of ca. 50 $\mu C\,cm^{-2}$) was chosen instead. As can be seen in Figure 2, at low concentrations the peak potential remains constant in all the cases, and equal to that in M^+-free 0.1 M H_2SO_4. Above a cation-dependent threshold concentration, the H_{upd} peak potential starts to deviate from the value in the absence of the cation and finally, at high enough concentrations, the peak potential decreases linearly with the logarithm of the cation concentration. This Nernstian-like behavior suggests that the cations are retained on the surface as $(CN_{ad})_x$-M^+ clusters in equilibrium with M^+ in the solution. As far as we know, this is the first example of a linear dependence of the equilibrium potential of an electrochemical reaction on the logarithm of the concentration of a species not involved in the reaction and which does not interact with the electroactive species, highlighting that non-covalent interactions can dramatically affect the double layer properties.

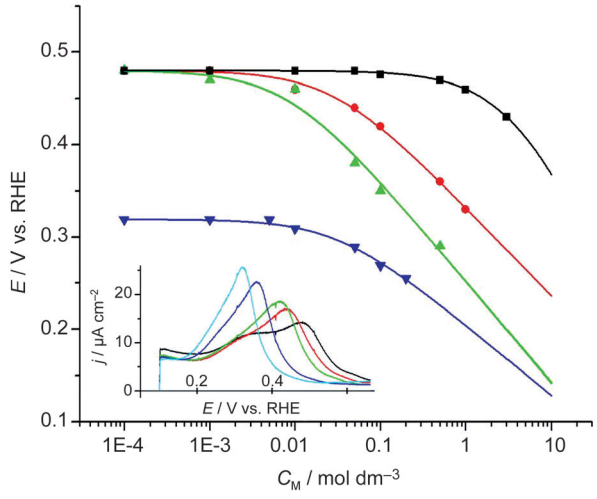

Figure 2. Semi-logarithmic plot of the dependence on the cation concentration of the peak potential for hydrogen adsorption on cyanide-modified Pt(111) electrodes in 0.1 M H_2SO_4 or $HClO_4$, as obtained from cyclic voltammograms at 50 $mV\,s^{-1}$. Black squares: Li^+; red circles: Na^+; green up triangles: K^+; blue down triangles: Cs^+. The lines correspond to the fit of the experimental data to Equation (2). Inset: Cyclic voltammograms in the H_{upd} region in 0.1 M H_2SO_4 containing Na^+ in different concentrations (red: 0.05 M Na^+; green: 0.1 M Na^+; blue: 0.5 M Na^+; cyan: 1 M Na^+).

This behavior can be easily modeled, assuming that the formation of the $(CN_{ad})_x$–H clusters can be represented by Equation (1):

$$H^+ + xCN_{ad} + ze \leftrightarrow (CN_{ad})_xH^{(1-z)} \quad (1)$$

and that the formation of the $(CN_{ad})_xM^+$ clusters can be described by the Langmuir isotherm. Then, the potential at which a given coverage of $(CN_{ad})_x$-$H^{(1-z)}$ clusters is attained will be given by Equation (2):

$$\begin{aligned} E &= E^0 + \frac{RT}{zF}\ln c_{H^+}(1-\theta_{M^+(CN)x}) \\ &= E^0 + \frac{RT}{zF}\ln c_{H^+} - \frac{RT}{zF}\ln(1+K_{M^+}c_{M^+}) \end{aligned} \quad (2)$$

where E^0 is the potential at which a given coverage of $(CN_{ad})_x$–H clusters is attained in the absence of cations at pH 0, K_{M+} is the equilibrium constant for the formation of the $(CN_{ad})_x$–M^+ clusters, z is the number of electrons crossing the interface per every $(CN_{ad})_xH$ cluster formed, and c_{M+} is the cation concentration in the solution [for a detailed deduction of Eq. (2), see the Supporting Information]. The model predicts that if $K_{M+}C_{M+} \ll 1$ (equivalently, $\theta_{M+(CN)x} \ll 1$), the peak potential is independent of the cation concentration. According to Equation (2), the threshold concentration above which the peak potential starts to decrease below that observed in the absence of cations will be the lower the higher the value of K_{M+}, that is, it will be a measure of the affinity of the cation for the CN_{ad} groups. When c_{M+} is high enough, $K_{M+}C_{M+} \gg 1$ (equivalently $\theta_{M+(CN)x} \approx 1$), and the potential decreases linearly with $\log c_{M+}$ with slope $2.3026RT/zF$. As can be seen in Figure 2, the fit of the experimental data to this model is excellent.

Table 1. Equilibrium constants for the formation of the $(CN_{ad})_x$–M^+ clusters (K_{M+}) and number of electrons crossing the interface per every $(CN_{ad})_xH$ cluster formed (z), as obtained from the fit of the experimental data in Figure 2 to the model described by Equation (2). The last two columns show the Gibbs energy of hydration (ΔG^0) and the ionic diameter of the cations.

	K_M [M^{-1}]	z	ΔG^0 [eV][19]	Ionic diameter [Å][19]
Li^+	0.24 ± 0.07	0.28 ± 0.07	−5.3	1.56
Na^+	34 ± 6	0.61 ± 0.04	−4.3	1.96
K^+	120 ± 50	0.54 ± 0.08	−3.5	2.66
Cs^+	31 ± 11	0.8 ± 0.1	−2.9	3.30

Table 1 shows the values of K_{M+} and z for these four alkali metal cations, as obtained from the corresponding fits to Equation (2). Based on the values of K_{M+}, the following affinity series, $Li^+ \ll Cs^+ = Na^+ < K^+$, can be constructed. A similar series ($Li^+ \ll H^+ < Cs^+ = Na^+ < K^+ \ll Mg^{2+} \ll Ca^{2+} < Ba^{2+} \ll La^{3+}$) was deduced by Rosasco et al.,[18] who also demonstrated, using ex situ Auger spectra, that cation exchange proceeds without loss or rearrangement of the CN adlayer. Furthermore, the results in Table 1 indicate that less than one electron crosses the interface per $(CN_{ad})_xH$ formed in the presence of Li^+, Na^+, K^+ and Cs^+, although the values for z are only approximate for Li^+, because there are very few experimental points in the region of linear decrease of the peak potential with increasing cation concentration.

The formation of the $(CN_{ad})_x$–M^+ clusters must be due to non-covalent electrostatic interactions of the charge-dipole or charge-induced dipole type between the negative end of the CN_{ad} dipole and the oppositely charged M^+. These interactions would be expected to be stronger the smaller the cation radius, but on the contrary, K_{M+} is seen to increase strongly from Li^+ to K^+ and to decrease again for Cs^+. This observation cannot be explained only by the decrease in the hydration energy with increasing cation radius (see Table 1), and suggests that additional stability of the $(CN_{ad})_xM^+$ cluster is provided by an optimal fit of the cation into a cavity formed by the CN groups, as in some [2]-cryptate inclusion complexes formed by macrobicyclic ligands and alkali metals.[19] The size of the cavity formed by the CN groups must be close to the atomic diameter of Pt (2.77 Å), and K^+ must therefore fit particularly well inside it (atomic diameter: 2.66 Å, see Table 1). Although Cs^+ has a lower hydration energy than K^+, it is too big to fit in the cavity, and therefore its K_{M+} is smaller. A similar dependence of the stability constant of [2]-cryptates complexes, with a maximum for K^+, was found when cryptand [2.2.2] (cavity diameter of 2.8 Å) was used as ligand.[19] This suggests that the interaction between the cation and the surface-anchored CN groups is not exclusively electrostatic.

The alkaline metal cations adsorbed on the CN_{ad} groups could be visualized in situ using high-resolution electrochemical scanning tunneling microscopy (EC-STM), but only in solutions containing the cation in concentrations lying on the linear region of Figure 2. This was to be expected, since although the $(CN_{ad})_xM^+$ clusters are in equilibrium with the cation in solution, in this concentration region $\theta_{M+(CN)x} \approx 1$, and the STM tip will always see a cation occupying a given site. At concentrations below the linear region in Figure 2, the cations change positions too fast for the scan rate typically used in constant-current STM experiments. Figure 3 shows STM images

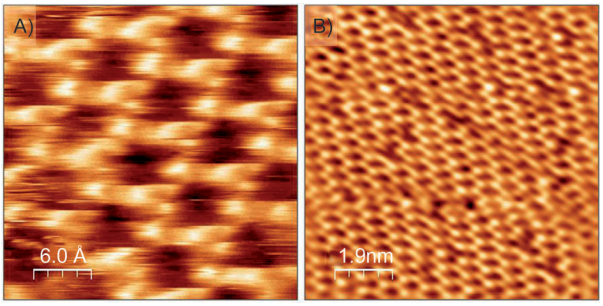

Figure 3. STM images of the honeycomb cation structure surrounding the CN rings ($I_T = 2$ nA). A) 3×3 nm^2 image of a cyanide-modified Pt(111) electrode in 0.1 M $HClO_4$ + 0.05 M $KClO_4$ at 0.60 V; $U_T = 0.45$ V (tip negative). B) 9.5×9.5 nm^2 image of a cyanide-modified Pt(111) electrode in 0.1 M $HClO_4$ + 0.5 M $NaClO_4$ at 0.55 V; $U_T = 0.3$ V (tip negative).

of a cyanide-modified Pt(111) electrode in acidic solutions containing K^+ (Figure 3A) and Na^+ (Figure 3B). The honeycomb structure shown in Figure 3 could only be observed for K^+ and Na^+ concentrations above 0.05 and 0.5 M, respectively. The same structure has been observed previously in the presence of Cu^{2+} at concentrations as low as 1 mM,[20] suggesting that in that case, the observed honeycomb structure was also due to the formation of $(CN_{ad})_x$–Cu^{n+} clusters. The low copper concentration sufficient for observing the honeycomb structure indicates a high affinity for the CN_{ad} groups of the copper cation.

As previously reported for copper, the honeycomb structures formed by potassium (Figure 3A) and sodium (Figure 3B) extend over the whole electrode surface. The observation of six tunneling maxima forming a honeycomb structure indicates that six M^+, located at the hexagon corners, surround every CN_{ad} hexagonal ring, forming $(CN_{ad})_3$–M^+ clusters. Location of the metal cation centred on the side of a hexagonal CN_{ad} ring, interacting with four CN_{ad} groups and forming $(CN_{ad})_4$–M^+ clusters, would yield a kagome structure, which is not experimentally observed. (Ball models of the honeycomb and the kagome structures can be found in the Supporting Information.)

The adsorption of Na^+ and K^+ onto the CN adlayer was also investigated by means of DFT calculations. In a first approximation, the adsorption energies of the cations on the different adsorption sites were calculated. For these calculations a low coverage approximation was used, that is, only one cation per unit cell was included. Three distinct *on-top* adsorption sites were examined: a site surrounded by three CN molecules, giving rise to $(CN_{ad})_3$–M^+, a site surrounded by four CN molecules, labeled as $(CN_{ad})_4$–M^+, and the center of the CN rings, to which we will refer to as $(CN_{ad})_6$–M^+. Table S1 of the Supporting Information summarizes the calculated binding energies, some relevant geometric parameters, and the Mulliken charge

analysis for these structures. The adsorption energies of each of the atoms on a 3×3 clean Pt(111) slab were also considered for comparison purposes, and the relevant results are also reported in Table S1 of the Supporting Information.

The binding energy of an atom on Pt(111) is notably increased by the presence of the CN adlayer. This is mostly due to the higher energy gain incurred by the electron withdrawn from the neutral atom upon its falling to the Fermi level of the metal, which is 2.86 eV lower for cyanide-modified Pt(111) than for Pt(111), and could be anticipated from the analysis of the electrostatic potential (see Supporting Information, Figure S2). According to the binding energies in Table S1 of the Supporting Information, the adsorption on the $(CN_{ad})_3$ site is slightly less favored than that on the $(CN_{ad})_4$ site, in contradiction with the experimental observation. For this reason, the honeycomb and kagome structures were constructed and optimized (see Supporting Information, Figures S7 and S8). Table 2 summarizes the calculated binding energies, some relevant geometric parameters, and the Mulliken charge analysis for these structures. For potassium, the calculated binding energies per cation are −5.62 and −5.42 eV for the optimized honeycomb and kagome structures, respectively. In the case of sodium, the adsorption energies per cation are −5.59 and −5.31 eV for the honeycomb and kagome geometries, respectively. The 0.2–0.3 eV gain in binding energy of the honeycomb structure results, at least in part, from avoiding M^+–M^+ repulsions.

Table 2. Bonding energies, some relevant structural parameters, and Mulliken charge analysis for the kagome and honeycomb structures for Na^+ and K^+ adsorbed onto the CN-modified Pt(111) surface.

	E_b [eV][a]	d(M^+–Pt) [Å][b]	d(N–M^+) [Å][c]	d(N–Pt) [Å][d]	δM^+ [e][e]	δCN [e][e]
M = Na^+						
kagome	−5.31	3.69	2.59	3.14	+0.88	−0.42
honeycomb	−5.59	4.23	2.43	3.14	+0.88	−0.32
M = K^+						
kagome	−5.42	3.86	2.65	3.14	+0.85	−0.40
honeycomb	−5.62	4.44	2.61	3.14	+0.90	−0.32

[a] Binding energy per M^+ atom referred to the optimized ($2\sqrt{3}\times 2\sqrt{3}$)$R30^\circ$CN adlayer and an M atom in the vacuum. [b] Distance between the cation and the Pt surface in the optimized structure. [c] Average distance between the cation and the nitrogen atom of the CN molecules surrounding the adsorption site. [d] Average distance from the N atoms of the adsorbed CNs to the Pt surface. [e] Mulliken charge of the species in the optimized structure.

In summary, we have used cyanide-modified Pt(111) electrodes to illustrate the importance of noncovalent interactions in governing the interaction between the cations present in the supporting electrolyte and the electrode surface, dramatically affecting the properties and structure of the electrochemical double layer. The insight drawn from the experimental and theoretical results presented here has allowed us to understand previously reported results regarding the positive shift by 0.20 V in the onset of hydrogen adsorption on cyanide-modified Pt(111) electrodes and regarding copper adsorption on cyanide-modified Pt(111) electrodes and suggests that non-covalent interactions with surface-anchored species can be used to obtain extended surface nanostructuring following a predefined motif. Remarkably, non-covalent interactions can induce a Nernstian-like dependence of the equilibrium potential on the concentration of a species not involved in the electrochemical reaction and which does not interact with the electroactive species. Finally, we have been able to visualize the cations retained on the electrode surface by non-covalent interactions using high-resolution in situ EC-STM, and hints regarding the stability of the structure observed as compared to other possible structures have been obtained from theoretical calculations. The model developed here to describe the interaction of alkali-metal cations with surface anchored CN groups might be of general applicability to explain previously observed cation effects on the properties of the electrochemical double layer.[5,6,21]

Experimental Section

Experimental details have been reported previously[13–16,20] and can be found in the Supporting Information. All the potentials in the text are referred to the RHE. DFT-based calculations were carried out using the SIESTA software.[22] More details regarding the theoretical methods employed can be found in the Supporting Information.

Acknowledgements

Funding from the DGI (Spanish Ministry of Science and Innovation) through Project CTQ2009–07017 is gratefully acknowledged. M.E.-E. acknowledges an FPI fellowship from the Spanish Ministry of Science and Innovation and an accommodation grant at the Residencia de Estudiantes from the Madrid City Council. N.M.M. acknowledges the support from the Director, Office of Science, Office of Basic Energy Sciences, Division of Materials Sciences, US Department of Energy, under contract No. DE-AC03-76SF00098.

Keywords: density functional calculations · electrochemical double layer · non-covalent interactions · platinum · scanning probe microscopy

[1] H. Lodish, A. Berk, S. L. Zipursky, P. Matsudaira, D. Baltimore, J. Darnell, *Molecular Cell Biology, 4th ed.*, W. H. Freeman, New York, **2000**.
[2] C. A. Schalley in *Analytical Methods in Supramolecular Chemistry* (Ed.: C. Schalley), Wiley-VCH, Weinheim, **2007**, pp. 1–16.
[3] D. Strmcnik, K. Kodama, D. van der Vliet, J. Greeley, V. R. Stamenkovic, N. M. Markovic, *Nat. Chem.* **2009**, *1*, 466.
[4] D. Strmcnik, M. Escudero-Escribano, K. Kodama, V. R. Stamenkovic, A. Cuesta, N. M. Markovic, *Nat. Chem.* **2010**, *2*, 880.
[5] J. M. Feliu, M. J. Valls, A. Aldaz, M. A. Climent, J. Clavilier, *J. Electroanal. Chem.* **1993**, *345*, 475.
[6] N. García, V. Climent, J. M. Orts, J. M. Feliu, A. Aldaz, *ChemPhysChem* **2004**, *5*, 1221.
[7] V. B. Paulissen, C. Korzeniewski, *J. Phys. Chem.* **1992**, *96*, 4563.
[8] C. S. Kim, C. Korzeniewski, *J. Phys. Chem.* **1993**, *97*, 9784.
[9] C. Stuhlmann, I. Villegas, M. J. Weaver, *Chem. Phys. Lett.* **1994**, *219*, 319.
[10] J. L. Stickney, S. D. Rosasco, G. N. Salaita, A. T. Hubbard, *Langmuir* **1985**, *1*, 66.
[11] Y.-G. Kim, S.-L. Yau, K. Itaya, *J. Am. Chem. Soc.* **1996**, *118*, 393.
[12] F. Huerta, E. Morallón, J. L. Vázquez, *Electrochem. Commun.* **2002**, *4*, 251.

[13] I. Morales-Moreno, A. Cuesta, C. Gutiérrez, *J. Electroanal. Chem.* **2003**, *560*, 135.
[14] A. Cuesta, M. Escudero, *Phys. Chem. Chem. Phys.* **2008**, *10*, 3628.
[15] A. Cuesta, *J. Am. Chem. Soc.* **2006**, *128*, 13332.
[16] A. Cuesta, M. Escudero, B. Lanova, H. Baltruschat, *Langmuir* **2009**, *25*, 6500.
[17] H. H. Rotermund, S. Jakubith, S. Kubala, A. Vonoertzen, G. Ertl, *J. Electron Spectrosc. Relat. Phenom.* **1990**, *52*, 811.
[18] S. D. Rosasco, J. L. Stickney, G. N. Salaita, D. G. Frank, J. Y. Katekaru, B. C. Schardt, M. P. Soriaga, D. A. Stern, A. T. Hubbard, *J. Electroanal. Chem.* **1985**, *188*, 95.
[19] J. M. Lehn, J. P. Sauvage, *J. Am. Chem. Soc.* **1975**, *97*, 6700.
[20] M. Escudero, J. F. Marco, A. Cuesta, *J. Phys. Chem. C* **2009**, *113*, 12340.
[21] C. Stoffelsma, P. Rodriguez, G. Garcia, N. Garcia-Araez, D. Strmcnik, N. M. Markovic, M. T. M. Koper, *J. Am. Chem. Soc.* **2010**, *132*, 16127.
[22] J. M. Soler, E. Artacho, J. D. Gale, A. García, J. Junquera, P. Ordejón, D. Sánchez-Portal, *J. Phys. Condens. Matter* **2002**, *14*, 2745.

Received: April 28, 2011
Revised: June 8, 2011
Published online on July 5, 2011

